First-principles study of preferential sites of hydrogen incorporated in epitaxial graphene on 6*H*-SiC(0001)

Bora Lee,[1] Seungwu Han,[1,*] and Yong-Sung Kim[2,†]
[1]*Department of Materials Science and Engineering, Seoul National University, Seoul 151-744, Korea*
[2]*Korea Research Institute of Standards and Science, P.O. Box 102, Yuseong, Daejeon 305-600, Korea*
(Received 7 December 2009; revised manuscript received 13 January 2010; published 23 February 2010)

The hydrogen (H) incorporation in the epitaxial graphene buffer layer on 6*H*-SiC(0001) with various H coverages is investigated using the density-functional method. The most stable site for a single H atom is on top of a threefold C atom in the graphene buffer layer, whereas the incorporation into the interfacial layer is less favored. However, when the H concentration is above 7.15×10^{14} cm^{-2}, the H atoms are more stable in the interfacial layer. This is because the H passivation of the SiC surface expands the spatial gap between the buffer layer and the substrate. This eventually results in the complete delamination of the graphene buffer layer from the SiC substrate at high H densities. The band structure indicates that the detached buffer layer is electronically close to the free-standing graphene layer. The present results suggest that the exfoliation of the buffer layer could be realized by injecting atomic hydrogen.

DOI: 10.1103/PhysRevB.81.075432 PACS number(s): 68.35.−p, 68.43.Bc, 81.05.ue

I. INTRODUCTION

Recently, graphene has attracted a broad interest for its unique electronic properties[1–4] and possible applications to nanoscale devices.[5] So far, several fabrication methods have been proposed that can be used to obtain a graphene monolayer. First, as a mechanical process, a single graphene layer can be detached from the graphite bulk using specific adhesives.[1] For large-scale synthesis and mass production, epitaxial growth methods have also been pursued, such as the graphitization of SiC surfaces[5–8] and annealing of Ni-carbon alloys.[9] In these methods, the thickness of graphene layers can be controlled by tuning growth parameters.[5,10]

When graphene is grown epitaxially on SiC, the first carbon layer from SiC forms covalent C-Si bonds with the underlying SiC substrate and is called the graphene buffer layer.[11] The second carbon layer that is grown on top of the buffer layer weakly interacts with the underlying structure, but its electronic structure is at variance with the isolated free-standing graphene sheet.[12,13] (For example, the band gap opens.) Therefore, the graphene layers must be completely decoupled from the substrate to ensure the electrical properties characteristic of the isolated graphene. One intriguing idea is to incorporate the hydrogen (H) atoms into the buffer layer, which may delaminate the buffer layer from the top of the H-passivated SiC substrate. The decoupled graphene layer would be similar to the free-standing one because the H-passivated SiC surface is chemically inert.

In fact, a few experimental studies have elaborated on hydrogenation of graphene. For example, Guisinger *et al.* tried to eliminate the surface and interface states by passivating the epitaxial graphene on SiC with atomic hydrogen.[14] However, the H atoms were easily bound at the graphene surface, rather than diffusing through the interfacial layer. When the mechanically cleaved graphene is hydrogenated, a hydrocarbon monolayer sheet, called the graphane, is formed.[15,16]

In this paper, we study the preferential atomic sites for the incorporation of H atoms into the SiC-graphene structure by carrying out the density-functional calculations on the graphene buffer layer on a 6*H*-SiC(0001) substrate. The site on top of a threefold C atom in the buffer layer is found to be the most stable location for a single H atom. However, the incorporation of H atoms into the interfacial layer is greatly enhanced at H densities larger than 7.15×10^{14} cm^{-2} as the graphene buffer layer is separated from the substrate. This results in the complete delamination of the buffer layer from the substrate.

II. COMPUTATIONAL METHODS

The density-functional calculations are performed using the VIENNA *ab initio* simulation package (VASP).[17] The ultrasoft pseudopotentials[18] are used with a kinetic energy cutoff of 300 eV, and the local density approximation (LDA) is used for the exchange-correlation energy.[19] For the surface Brillouin-zone (BZ) integration, (0, 0), (1/3, 2/3), and (2/3, 1/3) points (2×2 mesh) are sampled for each supercell, which corresponds to a 8×8 mesh including Γ and K points in the BZ of the 1×1 graphene unit cell. The atomic coordinates are relaxed until the Hellmann-Feynman forces are reduced to within 0.02 eV/Å.

The epitaxial graphene on the Si-terminated SiC(0001) surface typically exhibits a periodicity of $6\sqrt{3}\times6\sqrt{3}R30°$.[6] The study of the H adsorption in such a large cell is too costly, so we consider two smaller interfacial reconstructions, $\sqrt{3}\times\sqrt{3}R30°$ and 3×3, as shown in Fig. 1. In some experiments, the $\sqrt{3}\times\sqrt{3}R30°$ phase appeared before the $6\sqrt{3}\times6\sqrt{3}R30°$ reconstruction was stabilized.[5–8] In the $\sqrt{3}\times\sqrt{3}R30°$ cell, the SiC substrate is strained to match with the lattice parameter of the 2×2 unit cell of graphene (2.461 Å). This introduces a compressive strain of 7.8% in the SiC substrate. The carbon buffer layer is then formed by overlaying the 2×2 unit cell of graphene.[20] To study the H adsorption, a supercell is constructed by doubling the periodicity of the $\sqrt{3}\times\sqrt{3}R30°$ cell as shown in Figs. 1(a) and 1(c). For comparison, the 3×3 model in Figs. 1(b) and 1(d) is also studied. In this case, the SiC substrate is expanded by

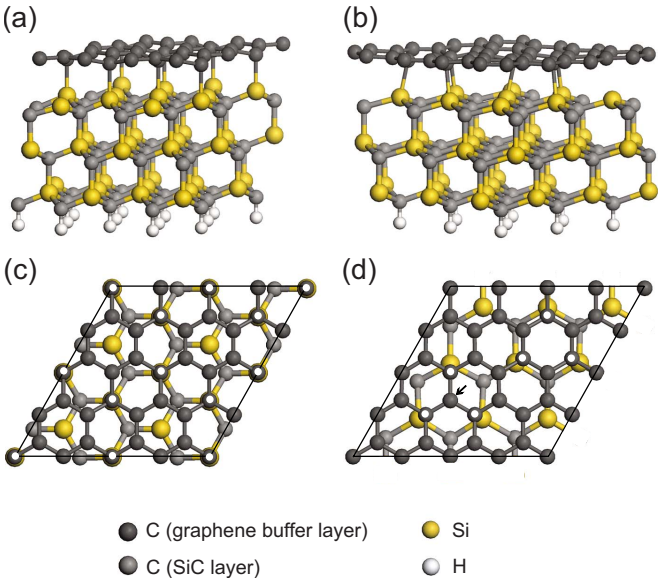

FIG. 1. (Color online) Atomic structures of the (a) $\sqrt{3} \times \sqrt{3}R30°$ and (b) 3×3 SiC-graphene models. (c) and (d) are the top views of (a) and (b), respectively. White dots indicate the four-fold C atoms forming an interfacial C-Si bond with the underlying SiC substrate.

6.5% to be commensurate with the 4×4 unit cell of graphene. As will be shown in the next section, the computational results for the two model structures qualitatively agree well, in spite of the opposing signs in the imposed strain. This indicates that the artificial strain introduced to match the lattice parameters do not affect main conclusions.

In both model structures, the substrate comprises three SiC bilayers. The C atoms at the bottom are passivated by H atoms [see Figs. 1(a) and 1(b)]. The length of the vacuum space is set to 15 Å. The atoms in the bottom SiC bilayer are fixed to the bulk positions to reduce the size effect from the finite layer thickness. In the following, we mainly discuss on the results for the $\sqrt{3} \times \sqrt{3}R30°$ model because its structure is closer to the experimentally observed $6\sqrt{3} \times 6\sqrt{3}R30°$ reconstruction, and the results for the 3×3 cell are discussed for comparison purposes.

III. RESULTS AND DISCUSSIONS

A. SiC-graphene structures

The interface binding energy of the $\sqrt{3} \times \sqrt{3}R30°$ SiC-graphene structure is calculated to be 0.57 eV per graphene primitive cell, which is similar to 0.72 eV from a previous study.[20] The small discrepancy could be attributed to the type of the pseudopotential (projector-augmented wave potential in Ref. 20 versus ultrasoft pseudopotential in the present work). At the interface, the SiC substrate contains four Si dangling bonds and eight interfacial C-Si bonds [the bonded C atoms are denoted by white dots in Fig. 1(c)]. The interfacial C-Si bond length is 1.972 Å, and the average distance from the buffer layer to the top-most Si layer is 2.264 Å. On the other hand, the interface binding energy in the 3×3 model is 0.29 eV per graphene primitive cell, which is much smaller than for the $\sqrt{3} \times \sqrt{3}R30°$ model. Consistently, the interfacial C-Si bond length is 2.017 Å which is larger than 1.972 Å in the $\sqrt{3} \times \sqrt{3}R30°$ model. At the interface, there are three Si dangling bonds and six interfacial C-Si bonds. Therefore, the density of the interfacial C-Si bonds is higher in the $\sqrt{3} \times \sqrt{3}R30°$ structure, and bond angles around Si atoms are also closer to the ideal tetrahedral value of 109.5° in the $\sqrt{3} \times \sqrt{3}R30°$ structure. This results in the stronger interfacial bond in the $\sqrt{3} \times \sqrt{3}R30°$ model compared to the 3×3 model.

TABLE I. Stable atomic sites and corresponding H incorporation energies (E_h) of a single H atom in the L0, L1, and L2 layers of the SiC-graphene $\sqrt{3} \times \sqrt{3}R30°$ and 3×3 structures. E_h^0 indicates the hydrogenation energies of the isolated graphene or 6H-SiC bulk.

Layer	Site	E_h (eV) ($\sqrt{3} \times \sqrt{3}R30°$)	E_h (eV) (3×3)	E_h^0 (eV)
L0	GR_s	−3.10	−3.82	−1.67
L1	DB_i	−2.50	−2.36	
	BC_i	−1.82	−2.45	
L2	AB_{DB}	−1.54	−2.61	
	AB_{Si}	−1.00	−2.76	0.17
	AB_C	−0.18	−0.38	0.35
	BC	−0.05	−0.65	0.40

B. Adsorption of single hydrogen

First, a single H atom in the SiC-graphene structure is considered. In order to compare the relative stabilities between different adsorption configurations, we define the average hydrogenation energy, E_h, for n H atoms considered in the supercell;

$$E_h = [E_{\text{SiC-GR-H}} - (E_{\text{SiC-GR}} + E_H \times n)]/n, \quad (1)$$

where $E_{\text{SiC-GR-H}}$, $E_{\text{SiC-GR}}$, and E_H are the total energies of the hydrogenated SiC-graphene, the hydrogen-free SiC-graphene, and a single isolated H atom (considering the spin-polarization), respectively. The binding energy of the H_2 molecule is 4.9 eV within the present computational scheme. (The experimental value is 4.52 eV.[21]) Therefore, if E_h is less than −2.45 eV, a chemical process leading to the specific adsorption configuration is exothermic when H_2 molecules are reactants. The various sites for the single H adsorption are compared in Table I. In the following, the details are discussed according to the layer into which the H atoms are introduced.

On the graphene surface (L0). The most stable site for the H atom on the surface of the buffer layer is on top of a threefold C atom (GR_s). In Fig. 1(c), these sites correspond to the C atoms in dark gray without white dots. The computed E_h is −3.10 eV and varies little between different GR_s sites. This is because all GR_s sites in Fig. 1(c) are symmetrically equivalent if one considers only the buffer layer and the first underlying SiC layer. The threefold C atoms do not bond

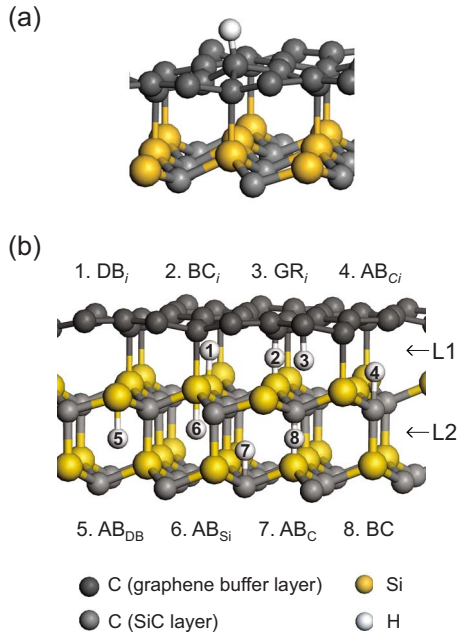

FIG. 2. (Color online) (a) The atomic structure of the single H atom adsorbed on a graphene buffer layer (GR$_s$), which is the most stable for a single H atom in the SiC-graphene structure. (b) Adsorption sites for the H atom in the L1 and L2 layers. See text for the detailed description.

with the substrate and therefore, retain a sp^2-like bonding configuration. However, due to the neighboring fourfold C atoms, the local configuration is slightly distorted from the ideal sp^2 geometry, rendering the threefold C atoms chemically active. When the H atom is attached to the GR$_s$ site, the C-H bond is formed with a length of 1.12 Å. As a result, the C atom becomes sp^3-like and protrudes above the buffer layer as shown in Fig. 2(a). On the other hand, the other adsorption sites in L0 are unstable. For instance, when the H atom is initially attached above a honeycomb hollow site, it spontaneously slides toward a nearby GR$_s$ site. A similar relaxation behavior is found for H atoms on top of a fourfold C atom or on the bridge sites between C-C bonds.

In both $\sqrt{3}\times\sqrt{3}R30°$ and $6\sqrt{3}\times 6\sqrt{3}R30°$ structures, every threefold C atom is neighbored by one fourfold C atom.[13] In contrast, the number of nearest fourfold C atoms in the 3×3 structure varies from 0 to 3 [Fig. 1(d)]. The computed E_h ranges over −3.82 to −1.67 eV and is approximately proportional to the number of neighboring fourfold C atoms. For example, the lowest value of −3.82 eV is obtained for the threefold C atom surrounded by fourfold C atoms [marked by an arrow in Fig. 1(d)], whereas the highest value of −1.67 eV corresponds to the adsorption site with all nearest C atoms in threefold configurations. This confirms that the local distortions induced by the fourfold C atoms mainly contribute to the chemical activity.

At the interface between graphene and SiC (L1). Figure 2(b) shows the adsorption sites available in the L1 layer. The interfacial dangling bond (DB$_i$) is on top of an unsaturated Si atom in the SiC surface. The interfacial bond center (BC$_i$) corresponds to the middle of the interfacial C-Si bond. For the graphene C-H bond at the interface (GR$_i$), the H atom is bonded to a threefold C atom from below. Lastly, the interfacial C antibonding (AB$_{Ci}$) site is on top of the C atom in the SiC surface. Among the four configurations, only the DB$_i$ and BC$_i$ sites are stable, with E_h of −2.50 and −1.82 eV, respectively. However, these sites are still less stable than the GR$_s$ sites in the L0 layer (−3.10 eV). The other sites, AB$_{Ci}$ and GR$_i$, are unstable, and the H atom moves to a nearby DB$_i$ site upon relaxation. In spite of the geometrical similarity to the GR$_s$ site, the GR$_i$ site is not preferred because the threefold C atoms in graphene protrude above the surface. The AB$_{Ci}$ site is unstable against the relaxation to DB$_i$ sites because the delocalized charges in the nearby Si dangling bonds strongly attract the H atom.

For the 3×3 structure, the E_h values for the most stable BC$_i$ and DB$_i$ sites are −2.45 and −2.36 eV, respectively. The energy difference between the two configurations is much smaller than for the $\sqrt{3}\times\sqrt{3}R30°$ structure. This is because the interfacial structure is less symmetric in the 3×3 model, and the relaxed geometries are similar whether the H atom is attached to the BC$_i$ or DB$_i$ sites. Some of AB$_{Ci}$ and GR$_i$ sites are found to be stable in the 3×3 structure with E_h of −2.19 and −1.76 eV, respectively.

Inside SiC (L2). The available sites in L2 are described in Fig. 2(b) as the antibonding of the Si atom with a dangling bond (AB$_{DB}$), Si antibonding (AB$_{Si}$), C antibonding (AB$_C$), and bond center (BC). The AB$_{Si}$, AB$_C$, and BC sites are named after the corresponding sites in cubic SiC.[22] The AB$_{DB}$ site is located under an unsaturated Si atom in the top SiC layer, passivating the Si dangling bond from the antibonding site. In Table I, it can be seen that AB$_{DB}$ is the most stable site in L2 with E_h of −1.54 eV. Therefore, E_h at any site in L2 is much higher than in L0 (−3.10 eV for GR$_s$) and L1 (−2.50 eV for DB$_i$). In the 3×3 structure, the E_h values for the AB$_{DB}$ and AB$_{Si}$ sites are −2.61 and −2.76 eV, respectively, which are significantly lower than the corresponding values in the $\sqrt{3}\times\sqrt{3}R30°$ structure. The tensile stress in the 3×3 structure might have facilitated the incorporation of the H atoms.

In comparison, the hydrogenation energy in the unstrained bulk 6*H*-SiC (E_h^0) is also calculated in the last column of Table I. The relative stabilities among adsorption sites are similar between the bulk and the L2 layer, but the lower values for the SiC-graphene system indicate that the H atoms can be incorporated more easily into the sub-surface region. In the 4*H*-SiC bulk, the AB$_{Si}$ site was found to be most stable for an interstitial H atom because the H atom is attracted to the positively charged Si atom.[23] Another more stable site, called the R site, was identified for 6*H*-SiC through the cluster calculations at the Hartree-Fock level.[24] However, this site could not be considered in the present model due to the small slab thickness.

C. Hydrogen pairs

Next, the adsorption of a pair of hydrogen atoms in the SiC-graphene structure is examined. Figure 3 shows possible configurations for the H pair with small separations. If two H atoms are located at the star-marked and 1NN sites in Fig. 3, the pair is called an orthodimer. Similarly, when the second

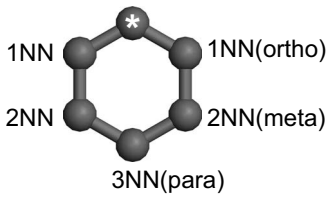

FIG. 3. Relative configurations of the paired H atoms on graphene. If the two H atoms are located at the star-marked and 1NN sites, the pair is called an orthodimer. Similarly, when the second H atom is located at the 2NN and 3NN sites, they are metadimer and paradimer, respectively.

H atom is adsorbed at the 2NN and 3NN sites, they are named as the metadimer and paradimer, respectively. In the $\sqrt{3}\times\sqrt{3}R30°$ structure, two H atoms in the pair are placed at different GR_s sites. We then consider various separations in the H pair up to 6NN, and compile the results in Table II. It is found that E_h varies slightly over the equivalent configurations because the symmetry of the buffer layer is lower than for the isolated graphene. Most of E_h values in Table II are close to that for the single adsorption at the GR_s site (−3.10 eV). Therefore, the pairing energy of the H atoms is negligible. For comparison, the E_h^0 values for the adsorption on the isolated graphene monolayer are shown in the third column of Table II. The orthodimer and paradimer are energetically most favorable, which is consistent with the scanning-tunneling microscope (STM) measurements of the H atoms on the graphite surface[25,26] or SiC(0001)-$(6\sqrt{3}\times 6\sqrt{3}R30°)$.[14] (Even though it was not mentioned explicitly, the graphene layer in Ref. 14 might not be the buffer layer.)

No meaningful tendency for H pairing is observed in the L1 and L2 layers, either. For example, two H atoms in the L1 layer are the most stable when they are attached at the DB_i sites with an E_h of −2.50 eV which is essentially the same as E_h for the isolated H atom at the DB_i site. A similar conclusion is reached for the adsorption in the L2 layer.

TABLE II. Hydrogenation energies (E_h) of the H pairs in L0. E_h^0 indicates the hydrogenation energies on the isolated graphene.

Pair structure	E_h (eV)	E_h^0 (eV)
1NN (orthodimer)	−3.11 to −3.10	−1.99
2NN (metadimer)	−3.13 to −3.11	−1.40
3NN (paradimer)	−3.04 to −2.68	−2.02
4 NN	−3.14	−1.67
6 NN	−3.11	−1.45

D. Hydrogen saturation

In this subsection, the hydrogenation behavior of the SiC-graphene structure is investigated as the H concentration is increased.

On the graphene surface (L0). In Fig. 4(a), the computed E_h is shown as the amount of H in L0 is increased. Within the unit supercell, the buffer layer contains 24 GR_s sites. When H atoms are adsorbed multiply, several configurations are considered for a given H concentration, and the one with the lowest total energy is presented in Fig. 4. It is seen that E_h does not change significantly until 12 H atoms are adsorbed in L0. Above this density, however, E_h increases, and it is −2.92 eV when 16 H atoms are attached. This value further increases to −2.38 eV when all of the 24 GR_s sites are occupied by H atoms.

The relaxed structures with 12 and 24 H atoms in L0 are displayed in Figs. 5(a) and 5(b), respectively. When more

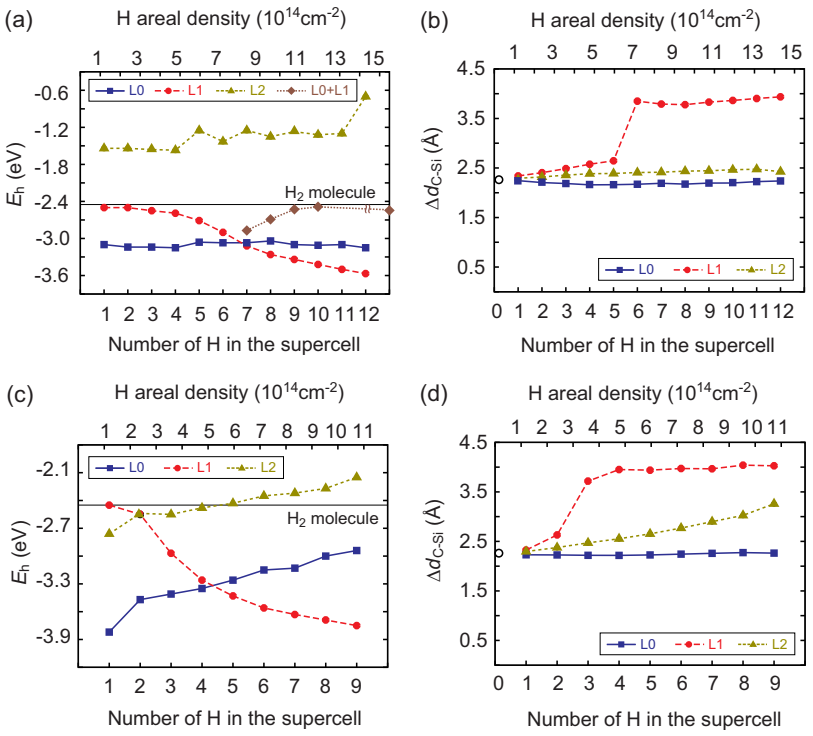

FIG. 4. (Color online) (a) Average hydrogenation energies (E_h) and (b) separations ($\Delta d_{C\text{-}Si}$) between graphene and the top-most Si layers of the $\sqrt{3}\times\sqrt{3}R30°$ structure. (c) and (d) are the corresponding plots for the 3×3 model. The open circles in (b) and (d) indicate interfacial separation without hydrogen. The horizontal lines in (a) and (c) indicate E_h of the H_2 molecule.

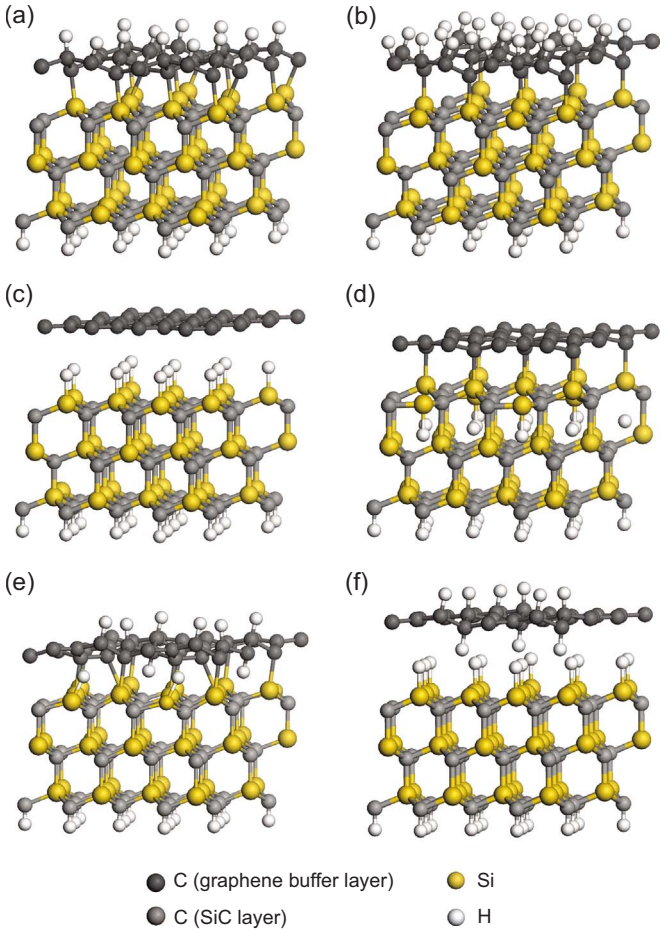

FIG. 5. (Color online) Atomic structures of the $\sqrt{3}\times\sqrt{3}R30°$ SiC-graphene structures with (a) 12 and (b) 24 H atoms in L0. (c) and (d) show the full saturation of H atoms in the L1 and L2 layers, respectively. (e) and (f) show the simultaneous incorporations into L0 and L1 layers. With 6 H atoms on the graphene surface, 4 and 12 H atoms are inserted into the L1 layer in (e) and (f), respectively.

than 12 H atoms are adsorbed, the steric interactions between the H atoms hinder the further adsorption and increase E_h. Furthermore, the puckering in the buffer layer becomes severe because the attached H atoms induce the sp^3 bonding. This results in a local geometry that is unfavorable for further H adsorption. In fact, when more than 24 H atoms are placed on L0, the additional H atoms are detached in the form of H_2 molecules because E_h is larger than that for the H_2 molecule (−2.45 eV).[27] Thus, the saturation limit of the H adsorption in L0 is estimated to be 24 H atoms or 2.86×10^{15} cm^{-2}. However, as will be discussed later, H atoms can be incorporated into the interface (L1) before the saturation limit is reached in L0. In Fig. 4(b), the average distance between the buffer layer and the top Si layer in SiC, $\Delta d_{C\text{-}Si}$, is plotted as a function of the H coverage. The separation does not change much even at the highest coverage.

Figure 4(c) for the 3×3 structure shows that E_h increases from −3.82 eV (1 H) to −2.94 eV (9 H). However, E_h levels off when more than 9 H atoms are attached; E_h for 11, 15, and 22 H adsorptions are −2.91, −2.93, and −2.88 eV, respectively. Further addition of H atoms at GR_s sites (there are 26 GR_s sites in the 3×3 structure) results in unstable C-H bonds due to the steric repulsion between the H atoms.

At the interface between graphene and SiC (L1). Up to the coverage of 5 H, E_h for the L1 layer does not change meaningfully [see Fig. 4(a)]. When one or two H atoms are considered, the H atoms prefer to attach at the Si dangling bonds (DB_i sites). Above this coverage, the H atoms start to break the C-Si bond by sitting at BC_i sites next to the H-passivated Si atoms, leaving sp^2-like graphene C atoms. As a result, the H atoms locally push graphene layer up, and monotonic dilation occurs around the H-passivated area as shown in Fig. 4(b).

Near the coverage of 5–6 H, noticeable changes are observed in both E_h and $\Delta d_{C\text{-}Si}$; E_h begins to drop more sharply [see Fig. 4(a)]. Concurrently, a large jump in $\Delta d_{C\text{-}Si}$ is noticeable in Fig. 4(b), meaning that the buffer layer is almost exfoliated and most interfacial C-Si bonds are broken. This generates many Si dangling bonds and the saturation of these bonds significantly lowers E_h. In addition, the more spacious interface facilitates the incorporation of additional H atoms.

The most interesting feature in Fig. 4(a) is that there is a crossover in the favored layer. When the coverage is larger than 6 H, the incorporation into the interface (L1) becomes energetically more stable than the adsorption on the graphene surface (L0). At the coverage of 12 H or 1.43×10^{15} cm^{-2}, all Si atoms at the interface are saturated, as four Si dangling bonds and eight BC_i sites are occupied by H atoms. The resulting structure is displayed in Fig. 5(c), which shows that the buffer layer is completely detached from the SiC substrate. E_h in this state is −3.57 eV, which corresponds to the lowest value found for the $\sqrt{3}\times\sqrt{3}R30°$ model. The band structure in the next section confirms that the exfoliated graphene layer is electronically identical to free-standing graphene.

The transition in the favored layer from L0 to L1 is also observed for the 3×3 structure, as can be seen in Fig. 4(c). The L1 layer in the 3×3 model contains nine interfacial Si atoms, three of which possess a dangling bond. The energetic stability switches from L0 to L1 when more than four H atoms are attached. The abrupt increase in $\Delta d_{C\text{-}Si}$ is also noted at this coverage [Fig. 4(d)]. The critical H density for the crossover is smaller than for the $\sqrt{3}\times\sqrt{3}R30°$ model because the interfacial bonding is weaker in the 3×3 model.

Inside SiC (L2). In the L2 layer, the H atoms passivate the interface Si dangling bonds at the AB_{DB} sites. However, the E_h value increases with the H coverage. This is because the strain energy is accumulated by the interstitial H atoms. Therefore, the incorporation of a large number of H atoms into the L2 layer is unlikely. A slight dilation is found as the H atoms are incorporated into the L2 layer [Fig. 4(b)]. A similar observation holds for the 3×3 structure in Figs. 4(c) and 4(d). Figure 5(d) shows the $\sqrt{3}\times\sqrt{3}R30°$ model with 12 H atoms incorporated into the L2 layer.

We also tested the multilayer hydrogenation for the coverage of 7–18 H in an aim to find more stable configurations. First, 6 H atoms are adsorbed on the GR_s sites because they are the most preferred sites for the coverage smaller than 7 H. The additional H atoms (up to twelve) are then incorporated into the L1 layer. The relaxed geometries in Figs. 5(e) (6 H in L0+4 H in L1) and 5(f) (6 H in L0+12 H in L1) show that some H atoms in L1 are stabilized on GR_i sites.

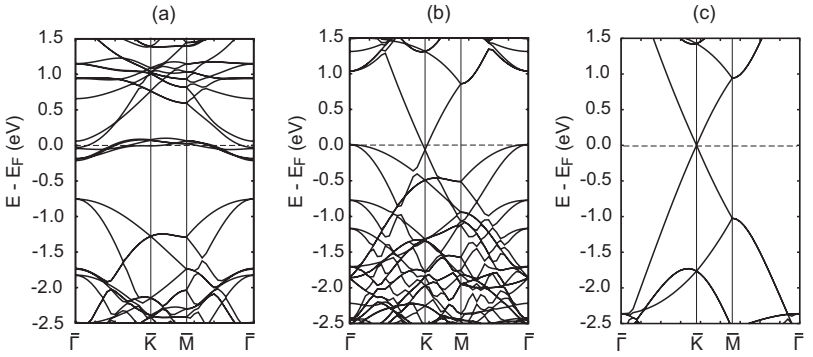

FIG. 6. Band structures of (a) the epitaxial graphene buffer layer on SiC, (b) graphene on the H-terminated SiC surface ($\sqrt{3}\times\sqrt{3}R30°$ model), and (c) the isolated graphene.

The corrugation in graphene may have increased the chemical activity of GR_i sites. In Fig. 4(a), E_h for the multilayer hydrogenation is shown as filled diamonds (the rightmost diamond is for when there are 12 H atoms in L1). It is found that the multilayer hydrogenation is less stable than the single layer hydrogenation in L0 or L1. Neither the large decrease in E_h nor the abrupt increase of $\Delta d_{C\text{-}Si}$ is observed for the multilayer hydrogenation. This result also indicates that the transition from L0 to L1, which is predicted in Fig. 4(a), is not likely to occur through the intermediate configurations such as Fig. 5(e) and 5(f).

E. Band structures

Finally, the band structure of the buffer layer on the 6*H*-SiC(0001) substrate is investigated. (See Fig. 6.) For the hydrogen-free $\sqrt{3}\times\sqrt{3}R30°$ structure, nondispersive bands are observed in Fig. 6(a) near the Fermi level. From the inspection of the wave functions, these bands are found to originate from the bottom and graphene buffer layers. For the fully delaminated structure in Fig. 5(c), the computed band structure is plotted in Fig. 6(b), and compared to the isolated graphene in Fig. 6(c). The linear dispersion near the $\bar{K}$ point is a hallmark feature for the isolated graphene. Thus, the electronic properties of the graphene layer that was split from the SiC surface are expected to be similar to the free-standing graphene. In Fig. 6(b), a slight electron doping is noted from SiC to the detached graphene. The biaxially compressive strain on the SiC substrate might be responsible for the electron transfer. For example, if one compares the valence top of hydrogenated SiC surfaces (without graphene), the value is 7.54 eV below the vacuum for the unstrained SiC while it reduces to 3.66 eV if the surface is strained as in this work. This is smaller than the work function of graphene (~4.5 eV) and therefore the electron transfer occurs from the strained SiC substrate to graphene. Considering that the surface band gap is smaller than the bulk band gap of 3.02 eV for 6*H*-SiC,[28] the conduction band minimum of the unstrained substrate would lie below the Fermi level of graphene and therefore, a small charge transfer from graphene to the SiC substrate is expected in the real situation.

IV. SUMMARY

In summary, we calculated various configurations of H adsorption and incorporation in the epitaxial graphene on 6*H*-SiC(0001). The most stable site for a single H atom was on top of a threefold C atom in the graphene buffer layer. The hydrogenation energy was higher when the H atom was incorporated in the interfacial layer or in the SiC substrate. The pair formation of H atoms was not preferred. As the H concentration increased, the hydrogenation energy on the graphene surface was more or less constant up to an areal density of 1.43×10^{15} cm^{-2}. However, the energy increased significantly above this concentration. On the other hand, in the interfacial layer, the hydrogenation energy monotonically decreased as the H concentration increased. This is because the H atoms in the interfacial region expanded the spatial gap between the graphene buffer layer and the substrate. As a consequence, the incorporation of H into the interface became energetically more favorable than the adsorption on the graphene surface when the H concentration is larger than 7.15×10^{14} cm^{-2}. Eventually, the graphene buffer layer completely delaminated from the H-terminated SiC substrate. The band structure of the detached graphene was identical to the isolated graphene. Based on the present computational results, we suggest that the exfoliation of a buffer layer from the SiC substrate could be realized in experiment if high densities of H atoms can be injected. However, the large energy barrier of H atoms to diffuse from the surface to the interface would pose a hurdle in the real situation. (In our calculation, the barrier is estimated to be 1.36 eV.) Therefore, the presence of surface holes or step edges together with the injection of atomic hydrogen would be essential to chemically detach the buffer layer from the SiC substrate.

ACKNOWLEDGMENTS

This work was supported by the Nano R&D program through the National Research Foundation of Korea funded by the Ministry of Education, Science, and Technology (Grant No. 2009-0082489) and Quantum Metamaterials Research Center (Grant No. R11-2008-053-03001-0). The computations were carried out at the KISTI Supercomputing Center (Grant No. KSC-2009-S03-0008).

*hansw@snu.ac.kr
†yongsung.kim@kriss.re.kr

[1] K. S. Novoselov, A. K. Geim, S. V. Morozov, D. Jiang, Y. Zhang, S. V. Dubonos, I. V. Grigorieva, and A. A. Firsov, Science **306**, 666 (2004).
[2] K. S. Novoselov, A. K. Geim, S. V. Morozov, D. Jiang, M. I. Katsnelson, I. V. Grigorieva, S. V. Dubonos, and A. A. Firsov, Nature (London) **438**, 197 (2005).
[3] Y. Zhang, Z. Jiang, J. P. Small, M. S. Purewal, Y.-W. Tan, M. Fazlollahi, J. D. Chudow, J. A. Jaszczak, H. L. Stormer, and P. Kim, Phys. Rev. Lett. **96**, 136806 (2006).
[4] M. I. Katsnelson, K. S. Novoselov, and A. K. Geim, Nat. Phys. **2**, 620 (2006).
[5] C. Berger, Z. Song, X. Li, X. Wu, N. Brown, C. Naud, D. Mayou, T. Li, J. Hass, A. N. Marchenkov, E. H. Conrad, P. N. First, and W. A. de Heer, Science **312**, 1191 (2006).
[6] I. Forbeaux, J.-M. Themlin, and J.-M. Debever, Phys. Rev. B **58**, 16396 (1998).
[7] J. Hass, R. Feng, T. Li, X. Li, Z. Zong, W. A. de Heer, P. N. First, E. H. Conrad, C. A. Jeffrey, and C. Berger, Appl. Phys. Lett. **89**, 143106 (2006).
[8] R. M. Tromp and J. B. Hannon, Phys. Rev. Lett. **102**, 106104 (2009).
[9] K. S. Kim, Y. Zhao, H. Jang, S. Y. Lee, J. M. Kim, K. S. Kim, J.-H. Ahn, P. Kim, J.-Y. Choi, and B. H. Hong, Nature (London) **457**, 706 (2009).
[10] T. Ohta, A. Bostwick, J. L. McChesney, T. Seyller, K. Horn, and E. Rotenberg, Phys. Rev. Lett. **98**, 206802 (2007).
[11] F. Varchon, R. Feng, J. Hass, X. Li, B. N. Nguyen, C. Naud, P. Mallet, J.-Y. Veuillen, C. Berger, E. H. Conrad, and L. Magaud, Phys. Rev. Lett. **99**, 126805 (2007).
[12] S. Y. Zhou, G.-H. Gweon, A. V. Fedorov, P. N. First, W. A. de Heer, D.-H. Lee, F. Guinea, A. H. Castro Neto, and A. Lanzara, Nat. Mater. **6**, 770 (2007).
[13] S. Kim, J. Ihm, H. J. Choi, and Y.-W. Son, Phys. Rev. Lett. **100**, 176802 (2008).
[14] N. P. Guisinger, G. M. Rutter, J. N. Crain, P. N. First, and J. A. Stroscio, Nano Lett. **9**, 1462 (2009).
[15] J. O. Sofo, A. S. Chaudhari, and G. D. Barber, Phys. Rev. B **75**, 153401 (2007).
[16] D. C. Elias, R. R. Nair, T. M. G. Mohiuddin, S. V. Morozov, P. Blake, M. P. Halsall, A. C. Ferrari, D. W. Boukhvalov, M. I. Katsnelson, A. K. Geim, and K. S. Novoselov, Science **323**, 610 (2009).
[17] G. Kresse and J. Hafner, Phys. Rev. B **47**, 558 (1993); **49**, 14251 (1994).
[18] D. Vanderbilt, Phys. Rev. B **41**, 7892 (1990).
[19] D. M. Ceperley and B. J. Alder, Phys. Rev. Lett. **45**, 566 (1980).
[20] A. Mattausch and O. Pankratov, Phys. Rev. Lett. **99**, 076802 (2007).
[21] K. P. Huber and G. Herzberg, *Molecular Spectra and Molecular Structure Constants of Diatomic Molecules* (Van Nostrand, New York, 1979).
[22] B. Aradi, A. Gali, P. Deák, J. E. Lowther, N. T. Son, E. Janzén, and W. J. Choyke, Phys. Rev. B **63**, 245202 (2001).
[23] M. Kaukonen, C. J. Fall, and J. Lento, Appl. Phys. Lett. **83**, 923 (2003).
[24] M. A. Roberson and S. K. Estreicher, Phys. Rev. B **44**, 10578 (1991).
[25] L. Hornekær, Ž. Šljivančanin, W. Xu, R. Otero, E. Rauls, I. Stensgaard, E. Lægsgaard, B. Hammer, and F. Besenbacher, Phys. Rev. Lett. **96**, 156104 (2006).
[26] L. Hornekær, E. Rauls, W. Xu, Ž. Šljivančanin, R. Otero, I. Stensgaard, E. Lægsgaard, B. Hammer, and F. Besenbacher, Phys. Rev. Lett. **97**, 186102 (2006).
[27] The detachment of hydrogen in the form of H_2 molecules was observed during the relaxation process, rather than molecular dynamics simulations. Therefore, the activation energy from the initial adsorption geometry to the final configuration with H_2 molecules should be very low, indicating the initial state was rather unstable.
[28] *Physics of Group IV Elements and III-V Compounds*, Landolt-Börnstein, New Series, Group III, Vol. 17 edited by O. Madelung (Springer-Verlag, Berlin, 1982) Part a.